Available online at www.sciencedirect.com
ScienceDirect
International Journal of Heat and Mass Transfer 51 (2008) 13–23
International Journal of HEAT and MASS TRANSFER
www.elsevier.com/locate/ijhmt

Experimental and numerical study of the heat transfer along a blunt flat plate

Ph. Marty [a,*], F. Michel [b], P. Tochon [b]

[a] Laboratoire des Ecoulements Géophysiques et Industriels, BP 53, 38041 Grenoble Cedex, France
[b] CEA-Greth, 17 Rue des Martyrs, 38054 Grenoble Cedex 9, France

Received 28 June 2006; received in revised form 15 March 2007
Available online 5 July 2007

Abstract

The development of light and efficient Compact Heat Exchangers (CHE) for automotive or aerospace applications has motivated recent research for the energetic optimisation of these devices. Owing to their geometrical complexity, such a goal requires valuable knowledges on the more simple case of a single plate in a fluid flow. The purpose of this study is to present an experimental and numerical study of the heat transfer between an incompressible fluid and a blunt flat plate with constant wall temperature. An experimental test rig is built in which air flows around a constant temperature copper plate. The Reynolds number defined on the plate thickness is varied from 120 to 500. Flow measurements are achieved with laser anemometry and the temperature field is determined using the cold wire technique. For each experiment, the experimental data are compared to Direct Numerical Simulations. Classical features of the flow are observed, i.e. a recirculating vortex near the leading edge of the plate, which is followed by a boundary layer from which vortices are alternately shed from both faces of the plate. Unlike previous studies, a particular attention is paid to the longitudinal distribution of the heat transfer coefficient for low to moderate Reynolds numbers. It is shown that a Direct Numerical Simulation of the flow and heat transfer around a thick plate is an efficient tool of optimisation which could be used for the design of industrial CHE.

Keywords: Heat transfer; Flat plate; Recirculating flow; Direct Numerical Simulation

1. Introduction

In view of the development of low-consumption energetic systems, the optimisation of Compact Heat Exchangers (CHE) becomes of crucial interest. Up to now, the increase of performances of such devices was not essential but the constant trend to lighter and more efficient exchangers has risen the importance of a better knowledge of the heat transfer behaviour between the flow and the fins. Prior to a detailed knowledge of the whole system with a complete account for the exact geometry of the exchanger, a first step consists of predicting the heat transfer along a single, isolated blunt flat plate immersed in an infinite flow. The geometry is shown in Fig. 1 where U_0 denotes the flow velocity at infinity, and e stands for the plate thickness. The Reynolds number $Re_{e/2}$ is hereafter defined with the half-thickness of the plate. One of the first detailed experimental studies about the flow structure is from Lane and Loehrke [1] who performed dye visualisation into a water channel. They report that a recirculating separation bubble forms at the leading edge. This bubble remains laminar for low Reynolds numbers and its reattachment length grows up to approximately $2l_r/e \approx 13$ for a Reynolds number close to 150. When the Reynolds number increases further, the recirculating bubble rapidly decreases and then keeps a constant value such as $2l_r/e \approx 9$. A view of the flow was given ten years later by Sasaki and Kiya [2] who made visualisation with hydrogen bubbles in a water experiment. They distinguished between three regimes:

* Corresponding author. Tel.: +33 4 38783286; fax: +33 4 38785360.
E-mail address: philippe.marty@hmg.inpg.fr (Ph. Marty).

0017-9310/$ - see front matter © 2007 Elsevier Ltd. All rights reserved.
doi:10.1016/j.ijheatmasstransfer.2007.04.036

Nomenclature

C_f	friction coefficient at the wall, $C_f = \frac{2\tau_w}{\rho U_0^2}$
C_P	pressure coefficient, $C_P = \frac{2(P-P_0)}{\rho U_0^2}$
e	thickness of the plate (m)
f	frequency of the vortices (Hz)
Gr_H	Grashof number, $Gr_H = \frac{g\beta\Delta T H^3}{\upsilon^2}$
H	width of the plate (m)
l_r	reattachment length (m)
L	length of the plate (m)
$Nu_{e/2}$	Nusselt number, $Nu_{e/2} = \frac{\bar{\varphi}}{\lambda\frac{T_w-T_0}{e/2}}$
Nu_x	local Nusselt number, $Nu_x = \frac{\varphi(x)}{\lambda\frac{T_w-T_0}{x}}$
P	pressure of the fluid (Pa)
P_0	pressure of the fluid at infinity (Pa)
Pr	Prandtl number of air
$Re_{e/2}$	Reynolds number of the flow, $Re_{e/2} = \frac{U_0 e}{2\upsilon}$
$St_{e/2}$	Strouhal number, $St_{e/2} = \frac{fe/2}{U_0}$
T_0	temperature of air at infinity (K)
T_w	temperature of the wall (K)
T_{mean}	time-averaged temperature of the fluid (K)
T_{rms}	root-mean square temperature of the fluid (K)
U_0	velocity of air at infinity (m s^{-1})
U^*	shear velocity such as $\tau_w = \rho U^{*2}$ (m s^{-1})
U, V	velocity components (m s^{-1})
x	axial coordinate along the plate (m)
y	distance from the wall (m)
y^+	dimensional distance from the wall, $y^+ = \frac{U^* y}{\upsilon}$

Greek symbols

υ	kinematic viscosity of air (m^2 s^{-1})
φ	heat flux density at the wall (W m^{-2})
Φ_{NC}	flux extracted by natural convection (W)
Φ_{FC}	flux extracted by forced convection (W)
ρ	fluid density (kg m^{-3})
τ_w	wall shear stress (Pa)
λ	thermal conductivity of air (W m^{-1} K^{-1})
Δx, Δy	size of the mesh in the x, y directions (m)

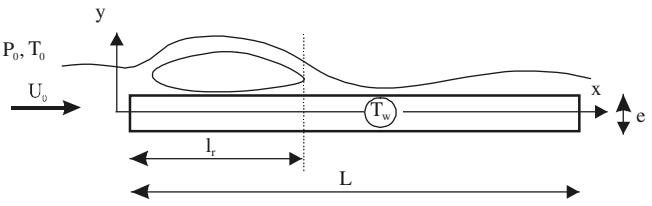

Fig. 1. Flow configuration on a blunt flat plate and coordinate system.

- For $Re_{e/2} < 160$, the reattachment length is laminar without any rolling up of the shear layer and no significant three dimensional effects are noticed.
- For $160 < Re_{e/2} < 190$, the shear layer rolls up owing to Kelvin–Helmholtz instabilities and Λ-shaped vortices are formed downstream of the reattachment point.
- For $Re_{e/2} > 190$, hairpin-like structures are formed and arranged in a staggered manner.

Their results are in agreement with previous works from Lane and Loehrke [1] and with those of Ota et al. [3] who made a complete study of the influence of the shape of the nose of a blunt plate by varying the angle of the leading edge.

From the papers which have been cited, it becomes clear that the flow on a blunt flat plate is completely different from the well known academic flow along an infinitely thin plate where no recirculating bubble appears.

In order to confirm the complexity of the flow it is worthwhile considering the evolution of the pressure all along the plate as another indicator of the reattachment phenomena. Various studies have been done for relatively high values of the Reynolds number (Chen et al. [4], Ota et al. [5], Hwang et al. [6]). All these studies show a sudden increase of the pressure between $2x/e = 6$ and 13. The central position of this pressure jump is located near $2x/e = 9$ what correspond to the reattachment length of the front vortex.

An alternative shedding of the vortices which are generated all along the plate occurs downstream of the plate. Quite similarly to what happens for the case of a flow past a transverse cylinder, the Strouhal number based on the plate thickness, e, remains almost constant. According to Okajima [7] who worked on a rectangular cylinder, the Strouhal number is approximately equal to 0.15.

Unlike flow studies which have considered both small and large values of the Reynolds number, the heat transfer along the plate has received attention for high Reynolds number flows only. The early paper from Ota and Kon [8] shows that the Nusselt number scales with $Re^{2/3}$. Their experiment consists of an electrically insulating plate on which a thin stainless steel foil is glued and then heated at constant heat flux by Joule effect. A first maximum of the heat transfer coefficient occurs near the leading edge where the shear layer is very thin. A second maximum appears near $2x/e = 8$ which is very close to the reattachment length which has been mentioned earlier and is also close to the location of the centre of the zone where the pressure increases. This increase in the heat transfer is the consequence of the flow of external fluid which is projected towards the plate through the boundary layer near the reattachment point.

Apart from these experimental works aiming at predicting the heat transfer along the plate, several numerical works are of interest. Owing to the computer limitations, the first attempts were limited to laminar flows with Reynolds number not greater than 50. Later, using the discrete vortices method, Kiya et al. [9] are the first to obtain a

numerical prediction of the reattachment length in agreement with the experiments at high Reynolds number ($Re_{e/2} = 13000$). They also report an increase of the heat transfer near the end of the recirculating bubble. Later, Tafti and Vanka [10,11], for Reynolds numbers up to 500, have used high performances computers to predict the full 2D and 3D unsteady flow along the plate. Surprisingly, they report that the 2D calculation contains most of the important features and behaviours of the full 3D calculation. However, no heat transfer results are given in their paper. Their work is completed soon after [12] by two-dimensional calculations performed at $Re_{e/2} = 500$ and a Prandtl number around unity. This has provided a deep insight of the vortex dynamics on the transport of a scalar quantity. Ten years ago, the Ω–Ψ technique was used by Kazeminejad et al. [13] to describe the heat transfer solution for Reynolds number below 160. It is only recently [14] that a full unsteady three-dimensional finite differences solution was published. In this paper, lateral walls are present in the spanwise direction, imposing a no-slip condition at the corresponding boundaries of the plate. It is shown that three-dimensional effects occur near the lateral edges of the plate but it is also shown that the central line located at mid-distance between the channel walls behaves quite similarly to what is observed in a pure 2D calculation.

After examining the literature, the following results can be listed:

- The knowledge of the flow along a flat blunt plate is well documented: various regimes are clearly identified as a function of the Reynolds number.
- In view of a future work on this problem, several criteria are available to assess the quality of the measurements or calculations which would be done: the reattachment length or the Strouhal number in the wake of the plate are also known functions of the Reynolds number.
- The heat transfer evolution along the plate is only known experimentally for high values of the Reynolds number: it has a maximum near the leading edge and another one near the reattachment point.
- Several 2D and 3D numerical calculations describe the flow and heat transfer along a blunt plate. Nevertheless, none of these works describe the downstream zone of the plate where the vortices are shed after they have left the trailing edge.

The aim of this work is then to investigate the heat transfer distribution in the regime of low Reynolds number ($100 < Re_{e/2} < 500$) which is representative of the industrial situation encountered in CHE. An experimental and a numerical approach are considered to allow a comparison between both methods. More precisely, the velocity measurements made on the experiment will be used to validate the computer technique which will be then used to study the heat transfer problem. The Section 2 of this paper presents the experimental apparatus which has been built to achieve the velocity and heat transfer measurements. Section 3 discusses the numerical tools and techniques which have been used for the computation. Section 4 presents the results and finally a conclusion is given.

2. Experimental setup

The aim of the facility which has been built was two fold:

- First of all, this facility should be able to help us in the validation of the numerical strategy which will be finally adopted, i.e., it should allow the measurement of velocity components in order to have access to the wall shear stress, the reattachment length of the recirculating bubble, the Strouhal number behind the plate.
- Secondly, it should be used to achieve thermal measurements to obtain informations on heat transfer between the plate and the fluid flow, i.e., it should permit temperature measurements in the fluid around the plate.

The experiment has been designed to provide an air flow at velocities between 0.3 m/s and 3.6 m/s, corresponding to Reynolds number $Re_{e/2}$ on the plate ranging from 50 to 600. The flow rate and the inlet temperature of the air flow are controlled in a PCV section having a cross section equal to 100×105 mm (Fig. 2). For each run, the inlet temperature is chosen such as it minimizes the influence of the natural convection, especially when the Reynolds number is low. Then, when $Re_{e/2}$ varies from 500 to 50, the inlet temperature varies from 40 °C to 20 °C. Meanwhile, the temperature difference between the fluid and the wall varies from 30 °C to 10 °C. For low Reynolds number, typically around 100, the free convection effects can become important when compared to forced convection effects: a quantitative estimation of the ratio of these two contributions will be presented in the section devoted to the experimental results. The air mass flow rate is measured via a Brooks 5853S mass flowmeter. A transparent perpex section has been included near the plate to allow laser velocity measurements. The plate is 5 mm thick and 75 mm long what gives a dimensionless length $2L/e = 30$. It is cooled by an inner flow of water. This cooled plate is located vertically in the centre of the air channel and is made of copper to ensure a constant temperature condition at the wall interface with the fluid. Owing to the important mass flow rate of the water flow, inlet and outlet temperatures are very close. Moreover, it has been checked that water temperature is extremely close to the plate surface temperature. Several K-type 0.5 mm thermocouples are located at various places of the facility to measure air and water temperature at the inlet and outlet of the facility. Apart from the velocity signal which is treated by the computer attached to the laser equipment, all signals are processed by a HP34970A acquisition unit. Around the plate, local temperature measurements are made using the classical cold wire technique allowing a precision of 0.1 °C on the temperature measurements. A special probe has been built with

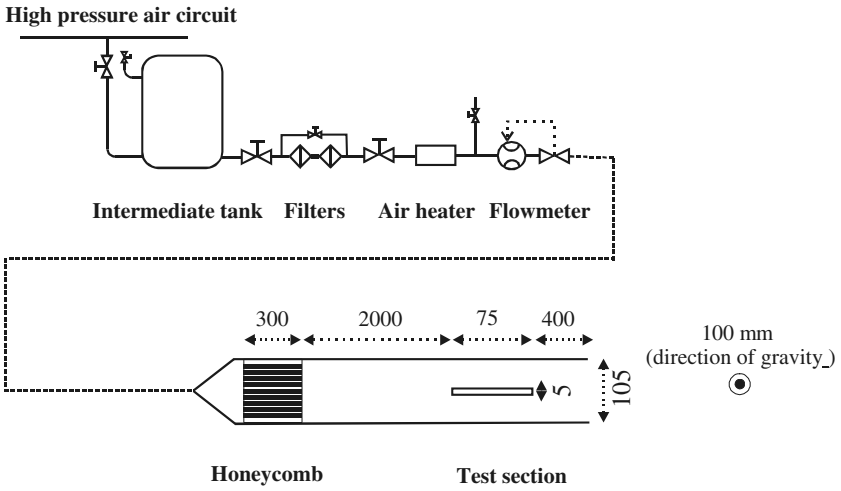

Fig. 2. Experimental facility (dimensions in mm).

a 1 μm wire mounted on a 1 mm support. A three-dimensional carriage allows a precise displacement of the laser beam and of the cold wire probe. The Nusselt number is measured from the knowledge of the temperature at the closest point near the wall: from the measurement of its distance to the wall together with the measurement of the water and air temperature, the wall heat flux density, and then the Nusselt number is obtained.

3. Numerical simulation of flow and heat transfer

Although the aim of this paper is the heat transfer problem for a single plate, our final goal is to model a network of several staggered plates arranged in the manner encountered in offset strip fin (OSF) heat exchangers. In this situation, one has to mesh several plates along the stream direction (typically 4–5) to render properly the Karman vortices interaction with the downstream plates. Similarly, at least 4–5 plates are necessary in the transverse direction to simulate an infinite array of plates. This geometry, which is composed from at least 16 plates, is accessible to 2D calculations but not realistic in three dimensions. This is the reason why we have restricted the computation of this paper to a 2D calculation, although we only deal here with a single plate. Nevertheless, as emphasized by Tafti [11], 2D calculations provide results close to fully 3D results. The same remark is made by Yanaoka [14] who has found that 2D computations are valid under the condition that the dimension in the spanwise direction is much greater (at least 10 times) than the plate thickness.

The computational strategy of this 2D calculation has been made by comparing the numerical results to a well documented case consisting of the flow around a plate for $Re_{e/2} = 360$, which is a typical value of the Reynolds number found in CHE used in cryogenic or automotive industry.

A finite volume computer code has been used for the Direct Numerical Simulation of the unsteady equations of continuity, momentum and energy and the computations have been done on a 2-processor Pentium Computer.

A two-dimensional regular mesh has been built in a 7.5×3 mm domain which is shown in Fig. 3 ($N_x \times N_y = 300 \times 120$, i.e. 36,000 cells). The plate dimensions are such that its dimensionless length $2L/e$ is equal to 30 as in our experimental facility. The mesh size is equal to 3 times the Kolmogorov scale, i.e. 0.025 mm. Such a mesh size corresponds to $y^+ = 3$ in wall units what means that the first computation point near the wall is located in the viscous sublayer. The wall receives a no-slip condition for the velocity and a constant temperature equal to 100 °C. Symmetry conditions are imposed on the upper and lower boundaries. An isothermal (0 °C) and constant velocity

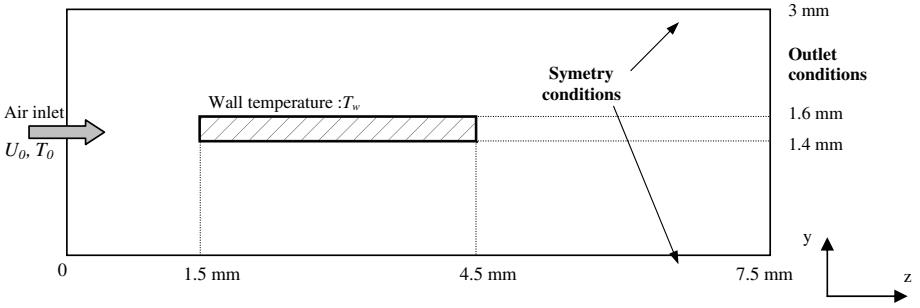

Fig. 3. Domain used for the numerical computation.

condition is imposed at the inlet of the domain (60 m/s; fluctuating component = 0). Free pressure Orlansky conditions are used at the outlet boundary of the calculation domain. This type of condition allows to evacuate vortices without disturbance. Moreover to fix the level of pressure at the outlet boundary, its value is imposed at the corners. The physical properties are independent of temperature.

Prior to running the code, several choices should be made concerning:

- The convective scheme for momentum and for energy.
- The temporal scheme for the time advancement procedure.
- The determination of the value of the time step.

For $Re_{e/2} = 360$, both upwind, centred and QUICK convective schemes have been tested for the discretisation of the momentum equations. A particular attention has been paid to the reattachment length, which is measured by detecting the position where the u_x component of the velocity changes its sign, but also to the Strouhal number in the wake of the plate: the results are shown in Table 1 in comparison to the literature and to our experimental data. It appears that the centred scheme is well adapted to our problem.

The time step satisfies the Courant and Fourier criteria and is defined as:

$$\Delta t = \frac{1}{\frac{1}{\Delta t_{\text{convection}}} + \frac{1}{\Delta t_{\text{diffusion}}}}$$

where $\Delta t_{\text{convection}}$ and $\Delta t_{\text{diffusion}}$ are such as:

$$\Delta t_{\text{convection}} = \frac{1}{\max\left(\frac{|u|}{\Delta x} + \frac{|v|}{\Delta y}\right)}$$

$$\Delta t_{\text{diffusion}} = \frac{1}{\max\left[2\nu\left(\frac{1}{\Delta x^2} + \frac{1}{\Delta y^2}\right)\right]}$$

Second and third order Runge-Kutta schemes as well as the Mac Cormack scheme have been tested for the temporal discretisation. Table 2 shows the results, again in comparison to the experimental results and the literature. Both the second and third Runge-Kutta schemes are acceptable: as it is faster, the RK2 scheme has been adopted in the following.

Table 1
Comparison of various convective schemes for momentum equations ($Re_{e/2} = 360$)

		Reattachment length $2l_r/e$	Wake Strouhal number $St_{e/2}$	CPU time
Convective scheme for momentum terms	Upwind	11.3	0.055	4.8 h
	Centred	9.3	0.085	7.8 h
	QUICK	17	0.075	9.7 h
Our experimental results		8	0.085	
Literature [1–3]		8–10	0.075–0.09	

Table 2
Comparison of various schemes for time advancement ($Re_{e/2} = 360$)

		Reattachment length $2l_r/e$	Wake Strouhal number $St_{e/2}$	CPU time
Temporal scheme	RK 2	9.3	0.085	7.8 h
	RK 3	9.3	0.083	10.6 h
	Mac Cormack	7	0.101	7.8 h
Our experimental results		8	0.085	
Literature [7]		8–10	0.075–0.09	

Finally, the scheme for the convective terms of the energy equation has been chosen by comparing the computed Nusselt number profile all along the plate to our experimental results. From the various schemes which have been tested (upwind, centred and QUICK) the QUICK scheme has been retained: the result is shown in Fig. 4 where the centred scheme is shown unstable near the end of the plate.

The final choices which have been made for the numerical computation are the following:

- Scheme for the convective term of the momentum equations: centred.
- Scheme for the convective term of the energy equations: QUICK.
- Scheme for time advancement: second order Runge-Kutta.

Fig. 5 shows a typical pattern of the temperature field when $Re_{e/2}$ is varied from 120 to 360. For $Re_{e/2} = 120$, the reattachment bubble is difficult to see but clearly appears near the leading edge for higher Reynolds numbers. Owing to its virtual insulation from the rest of the cold external fluid, this zone is subjected to poor heat exchange as it has been seen in Fig. 4, and, consequently is at a higher temperature than the rest of the boundary layer. Soon after the reattachment point, the boundary layer oscillates and its unsteadiness is at the origin of the Karman street in the wake.

The validation of the computational technique can also be discussed from Fig. 6 where, again for $Re_{e/2} = 360$, measured and computed velocity profiles have been plotted at equally spaced positions along the plate. In accordance to what has been mentioned earlier, negative velocities in the recirculating zone can be observed (Fig. 6a) for position such as $2x/e < 8$. Downstream, a slight thickening of the boundary layer is visible. Fig. 6b shows the profiles of fluctuations of the horizontal velocity. Here, unlike Fig. 6a where a fair agreement is observed between computation and experiment, some discrepancies can be found. Nevertheless, the value of the maximum of the fluctuations (around 10%) is rather well predicted.

A final validation of the numerical tool is shown in Fig. 7 which compares the computed profile of the pressure

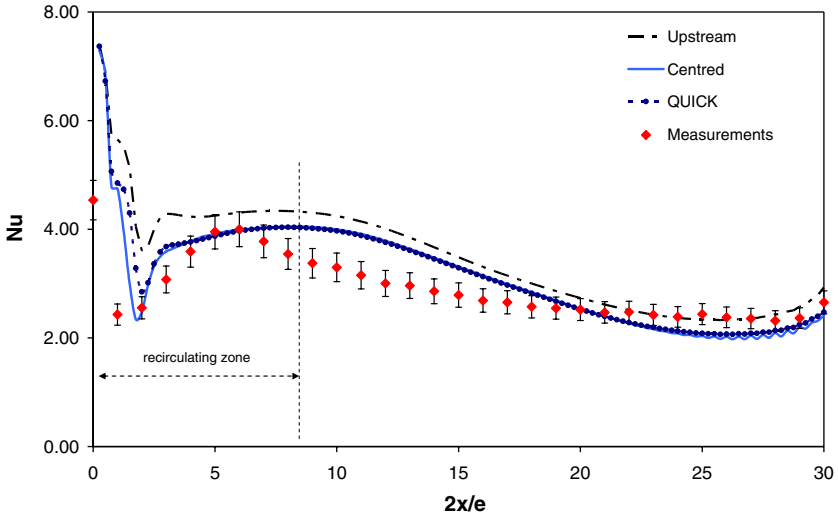

Fig. 4. Axial distribution of the Nusselt number for $Re_{e/2} = 360$: comparison between numerical results and experiments.

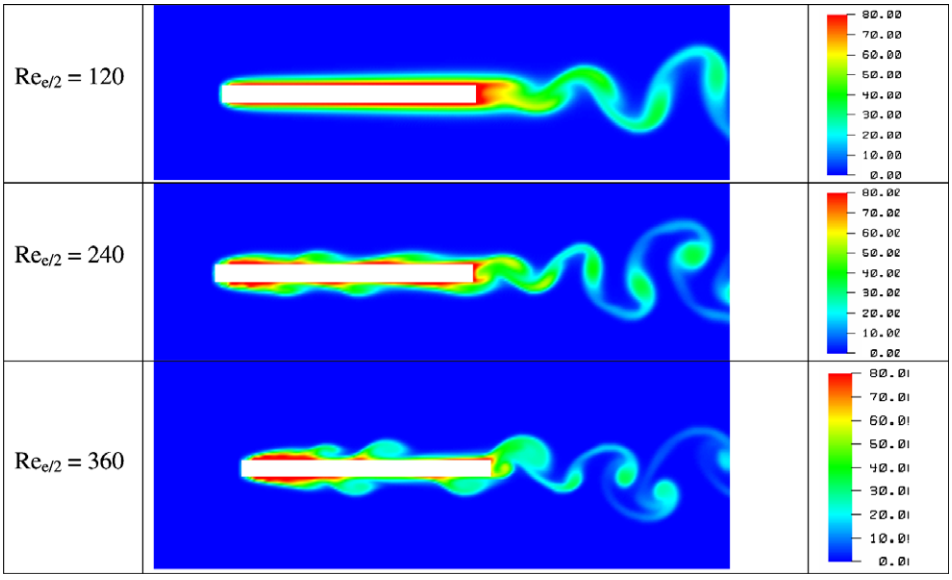

Fig. 5. Temperature contours for $Re_{e/2} = 120$, 240 and 360.

distribution to that from Hwang et al. [6]. It is most likely that the strong unsteadiness of the flow near the leading edge is responsible for the disagreement between experiments and simulation at the beginning of the plate. As a proof of this conjecture, Fig. 8, which shows computer results of the Strouhal number, shows a quite better agreement with our experiment on the one hand, but also with previous work from Okajima [7] on the other hand. This allows concluding that, despite the unsteady nature of the computer code, it is more easy to capture regular oscillations with a sharp spectrum as those which appear in the wake than the multiple frequency variations which occur in the reattachment zone. It is could be thought that an insufficient time-averaging is responsible for this disagreement: in this work, this averaging time was equal to 20 times the time needed for crossing the whole computational domain, i.e., equal to 45 times the typical period of the Karman flow instability.

At this point of the study, our numerical procedure has been validated for a particular value of the Reynolds number equal to 360. It can now be used for a comparison with experimental data for a wider range of Reynolds numbers: this will be done in the next paragraph.

4. Heat transfer results

The experimental facility has already been presented in Fig. 2. For a given Reynolds number, it allows cold wire measurement of the temperature in both normal and longitudinal direction. The copper plate which is used is 5 mm thick and 75 mm long what produce a dimensionless elongation factor $2L/e$ equal to 30: this value is the same as that

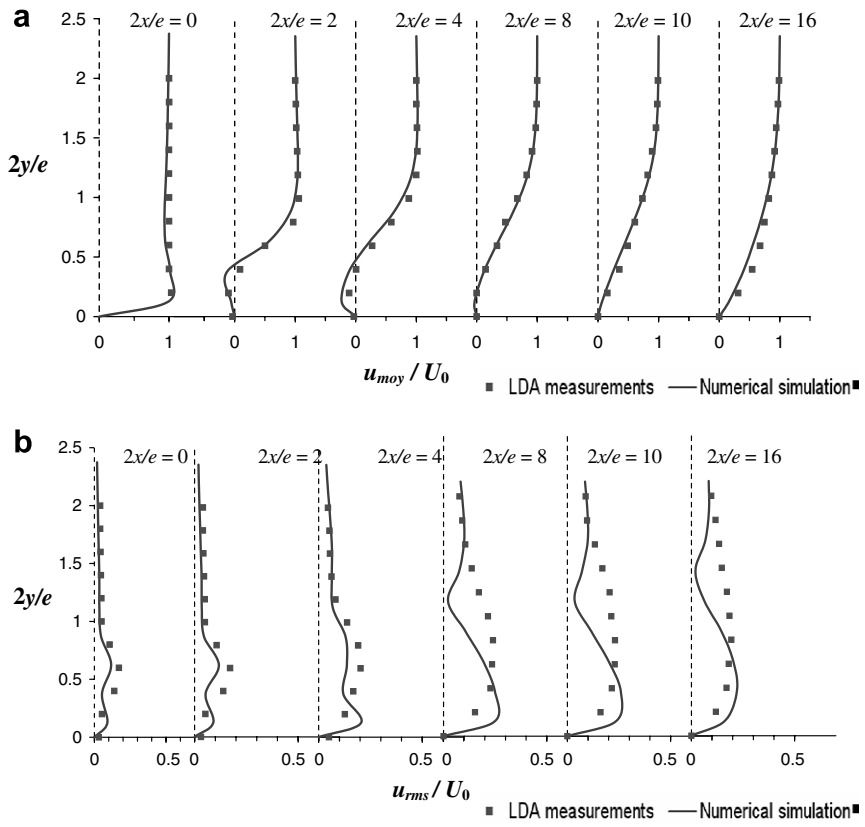

Fig. 6. Transverse profiles of horizontal velocity component U (a) and velocity fluctuations U_{rms} (b) for $Re_{e/2} = 360$. The plate extends from $2x/e = 0$–30.

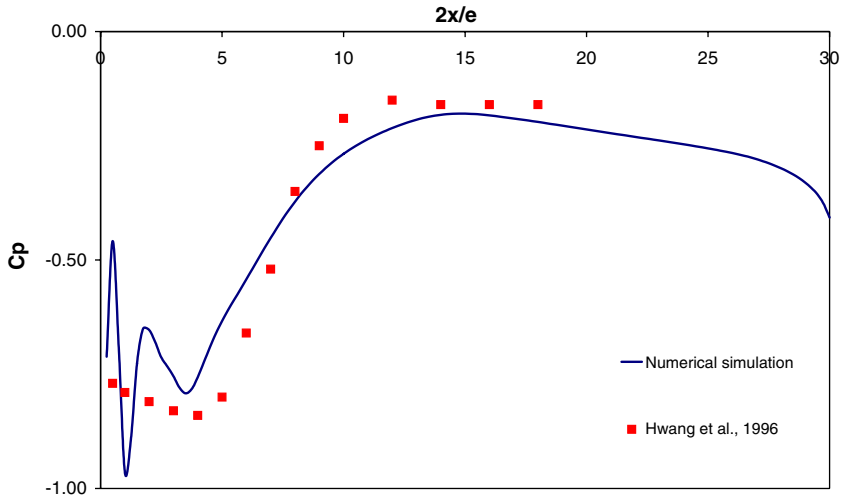

Fig. 7. Profile of the pressure coefficient for $Re_{e/2} = 360$: comparison between computer results and result from Hwang et al. [6].

used for the numerical computations. Before discussing the global heat transfer results and Nusselt numbers which have been obtained for various Reynolds numbers, it is worth paying attention to the details of the temperature distribution around the plate for the particular value $Re_{e/2} = 360$ which has received attention in our numerical study. Fig. 10a shows several temperature profiles plotted at different positions along the plate from $2x/e = 2$ to 16 (see Fig. 10b). For such a Reynolds number, as seen from Fig. 9, the reattachment length is equal to approximately 9. In the transverse direction, the first measurement point is located at 0.5 mm from the wall. The comparison between experimental data and numerical predictions is reasonable. We note that the thickness of the layer where the temperature differs from its value at infinity has a dimensionless value around 1.5.

The rms of the temperature fluctuations is shown in Fig. 11. The maximum of fluctuations is equal to

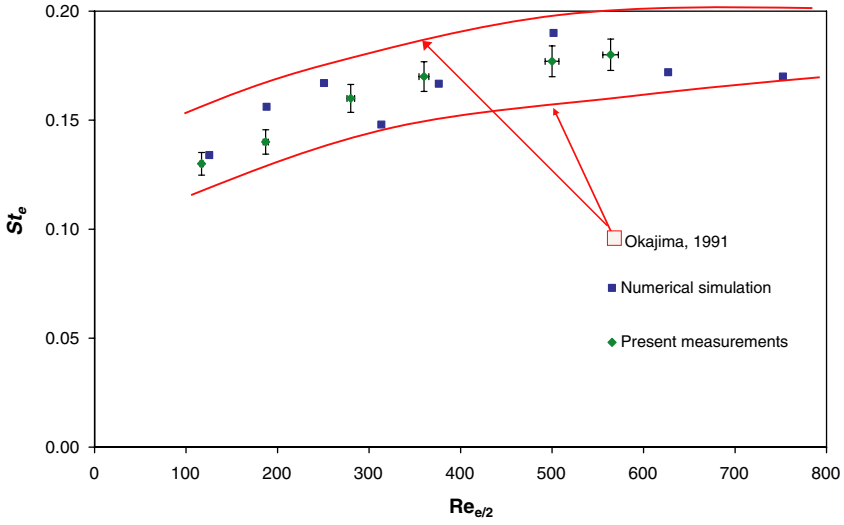

Fig. 8. Evolution of the Strouhal number with $Re_{e/2}$: comparison between our experimental and numerical results.

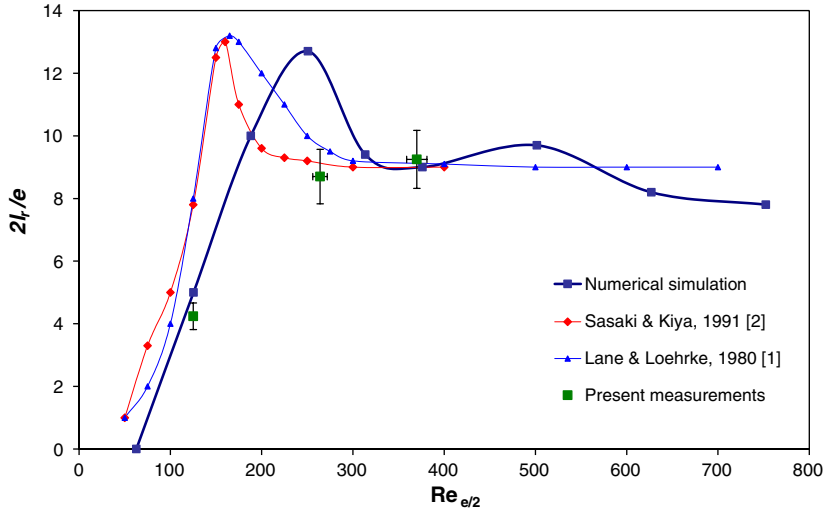

Fig. 9. Evolution of the reattachment length with the Reynolds number: comparison between our results and those from the literature.

approximately 10% and is reached at a dimensionless distance from the wall between 0.5 and 1. The agreement between experiment and simulation is again good although the thickness of the fluctuating zone is slightly greater in the experiment: this could be the consequence of a non negligible level of fluctuations in the flow entering the experimental test section. As a matter of fact, this turbulence level has been imposed to zero as an inlet boundary condition in the direct numerical simulation.

The profile of the Nusselt number along the plate is shown in Fig. 12 for three different values of the Reynolds number. For $Re_{e/2} = 120$, the agreement between experiment and computation is correct although the sharp peak of heat exchange which is reported from the computation is attenuated in the measurements. This may be the consequence of the diffusion of heat near the corner of the plate. It is interesting to compare the actual Nusselt number distribution to the well known solution for a laminar infinite plate which, in terms of the variables used in this work, becomes:

$$Nu_x = 0.332\left(\frac{2x}{e}\right)^{-1/2} Re_{e/2}^{1/2} Pr^{1/3}$$

For $Re_{e/2} = 120$, we see in Fig. 12a that a blunt plate almost behaves like an infinite plate. Fig. 12b and c show similar results for higher Reynolds numbers $Re_{e/2} = 360$ and 500. Although the Reynolds number based on the total length of the plate remains much smaller than the critical value of 10^5 at which turbulence arises, the agreement with the infinite laminar plate is now quite poor. This is the consequence of the unsteady nature of the recirculating bubble near the leading edge of the plate. As shown in an animated view of the computer results, the unsteadiness of this recirculating zone generates an intense incoming flux of external fluid near the reattachment point which, in turn, produces

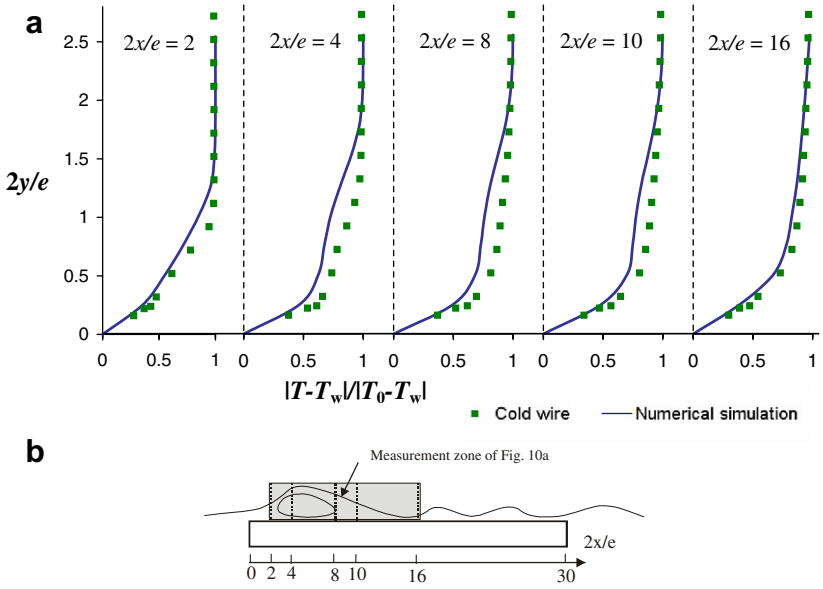

Fig. 10. (a) Transverse profiles of mean temperature at different locations and for $Re_{e/2} = 360$ and (b) corresponding measurement zone (the dotted lines represent the locations where the above profiles have been measured).

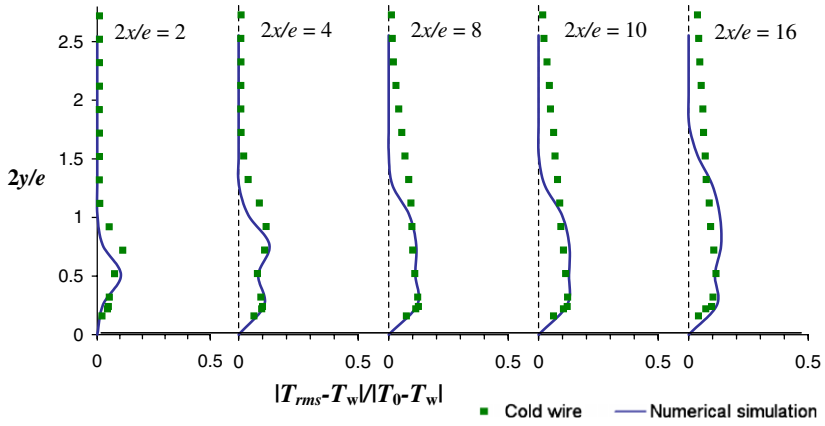

Fig. 11. Root-mean square of the temperature fluctuations along the plate at the same locations as in Fig. 10 and for $Re_{e/2} = 360$.

an increase in the heat exchange and Nusselt number. The situation is somewhat similar to a periodic jet which would hit the wall with a period equal to that of the boundary layer instabilities. As a consequence, the Nusselt number is greater near this impingement point than in the rest of the boundary layer.

Finally, it is interesting to discuss the global heat transfer coefficient on the whole plate. For $Re_{e/2} = 120$, 360 and 500, Table 3 shows the values of the mean Nusselt number $\overline{Nu}_{e/2}$ obtained by integration over the length of the plate. The values obtained for an infinite laminar plate are compared both to numerical and experimental results. We first note that the global agreement between simulation and experiment is better for the higher values of the Reynolds number and that the discrepancy is at most equal to approximately 10%. Here the influence of free convection should be discussed with the aim of forming the ratio $\frac{\Phi_{NC}}{\Phi_{FC}}$ of the heat which should be removed by natural convection alone to the heat which is removed by forced convection alone. This ratio will provide an exaggerated estimation of the influence of natural convection, probably higher than in the real mixed convection regime, but at least it will allow a rough estimation. According to Bejan et al. [15], the heat flux removed by free convection in air from a vertical plate is $Nu_H = 0.47 Gr_H^{1/4}$ where H is the plate height. A fit of the experimental results presented in Table 3 allows to express the Nusselt number of the forced convection phenomena: $Nu_{e/2} = 0.0078 Re_{e/2}$. For a facility working with air, this allows to form the ratio $\frac{\Phi_{NC}}{\Phi_{FC}}$:

$$\frac{\Phi_{NC}}{\Phi_{FC}} = \frac{3326 e \Delta T^{1/4}}{Re_{e/2} H^{1/4}}$$

where the three parameters e, ΔT and H have been intentionally left as variables. For the smallest value of the Reynolds number ($Re_{e/2} = 120$) this ratio is equal to 0.43 what illustrates a strong contribution of the natural convection. This ratio decreases to 0.1 for the higher value of Reynolds

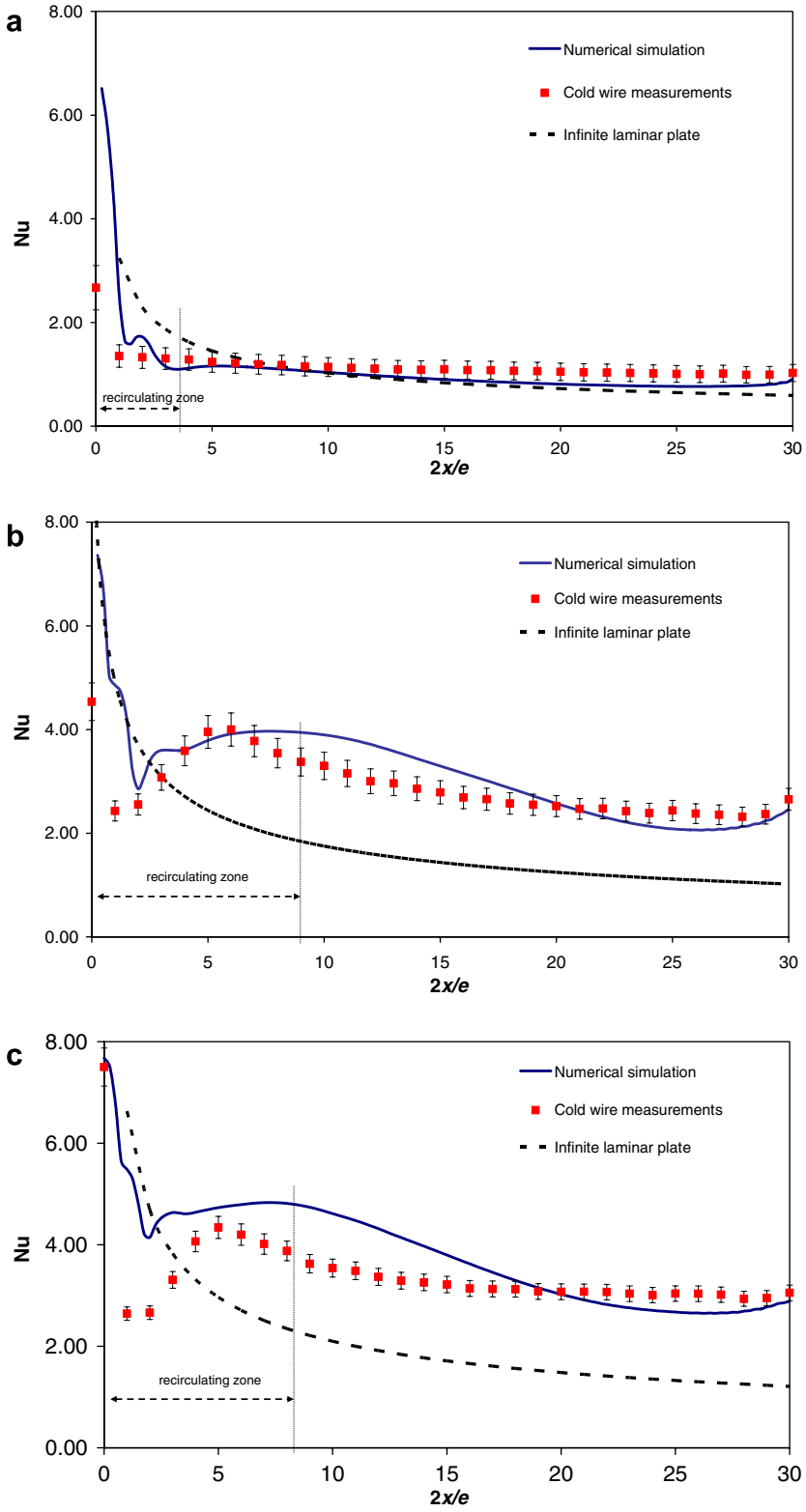

Fig. 12. Comparison between numerical and experimental profiles of the Nusselt number for various Reynolds numbers: (a) $Re_{e/2} = 120$. (b) $Re_{e/2} = 360$. (c) $Re_{e/2} = 500$.

($Re_{e/2} = 500$). At this point it is interesting to calculate what should be the value of the parameters e, ΔT or H which would have provided a relative effect of the natural convection less than 10% even for $Re_{e/2} = 120$. The value of e is 5 mm in our experiment and is not easy to diminish if a sufficient inner water circulation is required. The value of ΔT was 10 °C for the lowest value of Reynolds and should be reduced to 0.6 °C to reach $\frac{\Phi_{NC}}{\Phi_{FC}} = 10\%$. This is

Table 3
Global Nusselt number $\overline{Nu}_{e/2}$ as function of the Reynolds number: comparison between the infinite plate solution and the numerical and experimental results obtained on a finite length plate

	Infinite laminar plate	Numerical simulation	Experimental measurements	Agreement simulation/measurement
$Re_{e/2} = 120$	1.18	1.07	1.20	10.8%
$Re_{e/2} = 360$	2.05	3.14	3.00	4.4%
$Re_{e/2} = 500$	2.42	3.80	3.54	6.8%

not realistic as the error on the temperature measurements would become too large. Finally, the value of H which is 0.1 m in our experiment should be increased to 1.60 m to reach the 10% objective: although technically possible, this would require a much larger facility than that we have used. All this illustrate the difficulty to eliminate free convection effects at low Reynolds number.

From Table 3, we notice that the heat transfer enhancement brought by a blunt plate when compared to the infinite plate solution is almost negligible for $Re_{e/2} = 120$ but reaches 50% for $Re_{e/2} = 360$ and 500. This confirms the essential role of the boundary layer unsteadiness on the increase of the heat exchange between the wall and the fluid.

5. Conclusion

The heat exchange between a fluid and a flat blunt plate has been investigated numerically and experimentally for values of the Reynolds number between 120 and 500. The direct numerical simulation which has been undertaken shows that realistic results can be obtained in regimes where the unsteadiness of the flow is predominant. These results have been confirmed by experimental measurements on an air stream flowing around a constant temperature copper plate with an elongation factor $2L/e$ equal to 30. The main conclusions are:

- For small values of the Reynolds number ($Re_{e/2} = 120$), the recirculating bubble and the downstream boundary layer remain laminar. The recirculating zone reaches a maximum length around 13 when the Reynolds number is around 200. A Karman street is noticed in the wake with a Strouhal number $St_{e/2}$ around 0.065. The heat transfer is quite close to that observed for an infinite plate.
- When $Re_{e/2}$ increases, the boundary layer downstream of the recirculating zone first becomes turbulent. For higher values of the Reynolds number, the whole flow becomes unsteady. The unsteadiness of the front bubble is responsible for a pseudo-periodic impingement of external fluid which hit the wall and consequently locally increases the pressure coefficient and the heat transfer.
- For a Reynolds number around 500, the recirculating bubble reduces in size to a value around 9. The heat transfer is 50% higher than for an infinite plate.

From what has been presented here, it is concluded that current techniques of numerical simulations associated to nowadays capabilities of computers can be an efficient tool for the optimisation of industrial heat exchangers of the plate and fin type such as those used in the cryogenic industry. This allows thinking that the heat exchange between a fluid and a real network of fins could be predicted numerically with a sufficiently high precision: this would make easier the industrial optimisation of CHE.

Acknowledgement

This study was partially funded by the French Agency for Energy Saving (Ademe) which is thanked. The help on the TRIO code given by the Computing Department at CEA-Grenoble is also acknowledged.

References

[1] J.C. Lane, R.I. Loehrke, Leading edge separation from a blunt plate at low Reynolds number, ASME J. Fluid. Eng. 102 (1980) 494–496.
[2] K. Sasaki, M. Kiya, Three-dimensional vortex structure in a leading-edge separation bubble at moderate Reynolds numbers, J. Fluid. Eng. 113 (1991) 405–410.
[3] T. Ota, Y. Asano, J.I. Okawa, Reattachment length and transition of separated flow over blunt flat plates, Bull. JSME 24 (192) (1981).
[4] J.M. Chen, C.C. Chiou, Flow past a blunt flat plate subjected to the disturbance of incident vortex street, J. Wind Eng. Ind. Aerod. 66 (1997) 179–196.
[5] T. Ota, M. Itasaka, A separated and reattached flow on a blunt flat plate, ASME J. Fluid. Eng. 18 (1976) 79–86.
[6] K.S. Hwang, H.J. Sung, J.M. Hyun, Mass transfer measurement from a blunt-faced flat plate in a uniform flow, Int. J. Heat Fluid Flow 17 (1996) 179–182.
[7] A. Okajima, Change of flow about an elongated rectangular cylinder in a range of Reynolds numbers of 200 to 0.7×10^4, ASME, FED 112, Forum on turbulent flows, 1991, pp. 107–113.
[8] T. Ota, N. Kon, Heat transfer in the separated and reattached flow on a blunt flat plate, J. Heat Transfer 75 (1974) 459–462.
[9] M. Kiya, K. Sasaki, M. Arie, Discrete-vortex simulation of a turbulent separation bubble, J. Fluid Mech. 120 (1982) 219–244.
[10] D.K. Tafti, S.P. Vanka, A numerical study of flow separation and reattachment on a blunt plate, Phys. Fluid. A 3 (7) (1991) 1749–1759.
[11] D.K. Tafti, S.P. Vanka, A three-dimensional numerical study of flow separation and reattachment on a blunt plate, Phys. Fluid. A 3 (12) (1991) 2887–2909.
[12] D. Tafti, Vorticity dynamics and scalar transport in separated and reattached flow on a blunt plate, Phys. Fluid. A 5 (7) (1993) 1661–1673.
[13] H. Kazeminejad, M. Ghamari, M.A. Yaghoubi, A numerical study of convective heat transfer from a blunt flat plate at low Reynolds number, Int. J. Heat Mass Transfer 39 (1996) 125–133.
[14] H. Yanaoka, H. Yoshikawa, T. Ota, Numerical simulation of laminar flow and heat transfer over a blunt flat plate in square channel, Trans. ASME 124 (2002) 8–16.
[15] A. Bejan, A.D. Kraus, Heat Transfer Handbook, Wiley, 2003.